

promoting access to White Rose research papers



Universities of Leeds, Sheffield and York
<http://eprints.whiterose.ac.uk/>

This is an author produced version of a paper accepted for publication in **Indoor and Built Environment**.

White Rose Research Online URL for this paper:

<http://eprints.whiterose.ac.uk/78929/>

Paper:

Gilkeson, CA, Noakes, CJ and Khan, MAI (2014) *CFD Modelling and Optimisation of an Upper-Room UVGI System in a Naturally Ventilated Hospital Ward*. Indoor and Built Environment. (in press).

CFD Modelling and Optimisation of an Upper-Room UVGI System in a Naturally Ventilated Hospital Ward

C. A. Gilkeson^{1*}, C. J. Noakes², M. A. I. Khan²

¹*Institute of Engineering Thermofluids Surfaces and Interfaces, School of Mechanical Engineering,
University of Leeds, Leeds, United Kingdom, LS2 9JT*

²*Pathogen Control Engineering Institute, School of Civil Engineering, University of Leeds, Leeds, United
Kingdom, LS2 9JT*

*Corresponding author: C.A.Gilkeson@leeds.ac.uk

Abstract

Ultraviolet Germicidal Irradiation (UVGI) has been shown to be an effective technology for reducing the airborne bioburden in indoor environments and is already advocated as a potential infection control measure for healthcare settings. However, much of the understanding of UVGI performance is based on experimental studies or numerical simulation in mechanically ventilated environments. This study considers the application of an upper-room UVGI system in a naturally ventilated multi-bed hospital ward. A CFD model is used to simulate a Nightingale-type hospital ward with wind-driven cross-ventilation and three wall-mounted UVGI fixtures. A parametric study considering fifty different fixture configurations and three ventilation rates was carried out using a Design of Experiments (DoE) approach. Each configuration was assessed by calculating the UV dose distribution over the ward and at each bed. Results show that dose is influenced by the location of the fixtures and the ventilation regime. Thermal effects are likely to be important at low ventilation rates and may reduce UV effectiveness. A metamodel-based numerical optimisation was applied at a ventilation rate of 6 air changes per hour (ACH). In this case the optimum result is achieved when UVGI fixtures are mounted on the leeward wall at their lowest mounting height.

Keywords – CFD; UVGI; airborne infection; hospital ward; natural ventilation; numerical optimisation

Introduction

The airborne transmission of pathogens including tuberculosis and influenza poses a significant threat to human health [1,2]. This is a particular risk in healthcare settings such as hospital wards, where both infectious individuals and patients with weakened immune systems may be in close proximity; airborne transmission has been associated with a number of hospital outbreaks [3-5]. Conventionally, environmental control of airborne infection is accomplished through increasing ventilation rates to dilute and extract airborne pathogens and setting up ventilation systems to deliver appropriate pressure relationships between spaces [6]. However there is increasing awareness of the relationship between ventilation rate and energy consumption; up to 44% of energy in UK hospitals is thought to be consumed by ventilation and space heating [7]. Studies have suggested that air cleaning technologies may offer the potential to reduce airborne infection risk without the energy costs associated with higher ventilation rates [8,9].

One such strategy, upper-room Ultraviolet Germicidal Irradiation (UVGI) was developed for use in healthcare facilities long before antibiotics gained widespread use [10,11]. These systems use ceiling or wall mounted lamps to produce an irradiance field which is limited to the upper air zone in the room, above the heads of occupants. Airborne microorganisms from the occupied zone can be transported to the upper-zone by ventilation flows and convection currents, passing the microorganisms through the UV field. Exposure of microorganisms to UV-C light at a wavelength close to 254 nm, damages the microorganism DNA; at a sufficient dose this can be lethal, effectively killing the microorganism [12]. Several experimental studies have verified the disinfection performance of UVGI for a range of microorganisms in various settings [13-16], and a recent study conducted in clinical setting demonstrated a 70% reduction in TB transmission risk following the installation of an upper-room UVGI system [17]

One of the major difficulties of implementing upper-room UVGI systems is that the disinfection performance relies on the room airflow patterns which are responsible for transporting the microorganisms through the UV field. It therefore follows that the position of the UVGI fixtures and their interaction with the room ventilation is the dominant factor for maximising disinfection. Computational Fluid Dynamics (CFD) modelling has been shown in recent years to be a valuable tool for understanding the interaction between airflows and upper-room UVGI devices. Studies have simulated microorganism inactivation through scalar transport [16, 18, 19, 20] and particle-tracking [21] methods as well as considering the UV dose delivered by upper-room devices [22, 23]. Studies have also shown relationships with a ventilation system [19-22] potential to reduce cross-infection between patients [18] and the benefits of utilizing a mixing fan in conjunction with UV lamps [15, 24]. While these studies all yield insight into the factors influencing performance of UV systems, they simulate relatively small rooms which are mechanically ventilated. Upper room UVGI systems are often implemented in naturally ventilated environments, where the interactions between the UV field and the airflow patterns are largely unknown. The aim of this investigation is to simulate an upper-room UVGI system within a multi-bed naturally ventilated hospital ward and investigate how combining CFD analysis

with numerical optimisation tools can aid the design of such a system. The study focuses on a Nightingale-style ward with wind-driven cross-ventilation supplied via opening windows [25]. A CFD approach is used to simulate the wind-driven airflow patterns and to predict the UV dose arising from the placement of upper-room devices. The study also considers how a design of experiment technique can be used to efficiently conduct a parametric study considering device placement and ventilation rate, and how metamodel-based numerical optimisation methodology can be applied to evaluate the most suitable design option. Results are also presented to illustrate the potential impact of heat sources on the mixing and hence UV effectiveness under different ventilation conditions.

Methodology

Geometry, Mesh and Boundary Conditions

Figure 1 shows the geometry of the hospital ward used in the study which was generated using Gambit (version 2.4). The ward measures 7.2m wide, 3.4m high and 10.5m long (including a small corridor extension) leading to a volume of 200m³. The model is based on a section of real ward at St. Lukes Hospital in Bradford, UK [25].

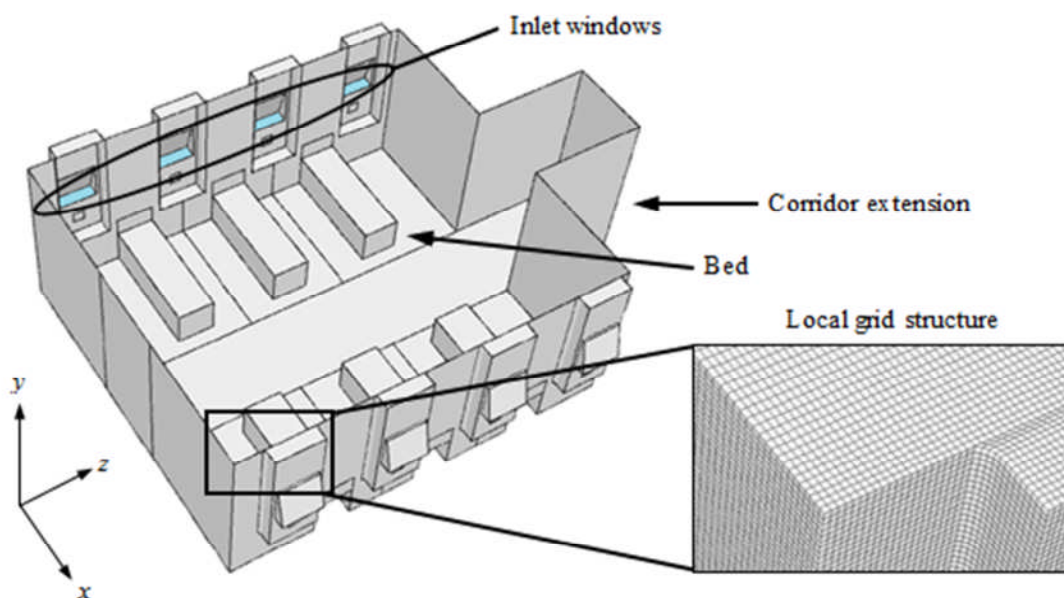


Figure. 1 Geometry of the six-bed Nightingale hospital ward used in the computations.

The modelled ward contains six simplified beds, three per side wall and ventilation is supplied via four open casement-type windows each supplying air at an inlet angle of 75° with respect to the horizontal axis. Cross ventilation is assumed with fresh air entering the four windward openings using velocity inlet boundary conditions before exiting through the four matching leeward openings which are defined as pressure outlets. This was selected over outflow condition as it enabled more stable convergence and the value of -5Pa (Table

1) was based on measured data [25]. The flow direction through each 0.8m x 0.2m inlet matches the angle of the windows; this behaviour was verified during an experimental study [25] and is shown in Figure 6. Simulations were carried out for three ventilation rates of 2, 6 and 12 ACH by applying corresponding velocity inlet conditions of 0.146 m/s, 0.438 m/s and 0.876 m/s respectively. These rates were selected to explore a range of realistic ventilation conditions that could be achievable in naturally ventilated wards. UK hospital design guidance recommends 6 ACH for ward areas [6], and by selecting substantially lower and higher rates, the influence of ventilation can be evaluated. Our experimental measurements reported in [25] show rates between 3.4-6.5 ACH with three windows per side open, depending on external wind conditions. Other studies in large naturally ventilated wards have shown higher rates over 12 ACH [26,27]. Turbulence intensity was based on a best estimate from anemometry measurements [25]. The simulation parameters and boundary conditions used in the study are summarised in Table 1.

Simulation setting/parameter	Details
Cell count	9416764
Turbulence model	RSM
Wall functions	Standard
Discretisation	2nd order
Gradient method	Green-gauss cell based
Inlet boundary condition (2ACH)	Velocity inlet, 0.146 m/s; Turbulence intensity = 10%; Hydraulic diameter = 0.3745 m
Inlet boundary condition (6ACH)	Velocity inlet, 0.438 m/s; Turbulence intensity = 10%; Hydraulic diameter = 0.3745 m
Inlet boundary condition (12ACH)	Velocity inlet, 0.876 m/s; Turbulence intensity = 10%; Hydraulic diameter = 0.3745 m
Outlet boundary condition	Pressure outlet, pressure = -5 pa

Table 1. Simulation parameters and boundary conditions

A recent computational study on a very similar geometry showed that grid independent solutions for the airflow patterns could be obtained using structured hexahedral cell sizes of 0.035m with span-wise grid stretching and local refinement around the window openings [28]. The results from this study showed that the discretisation error in the velocity magnitude varied between 0.38% and 3.40%, with the higher errors on the windward side of the ward. These errors were determined using the Grid Convergence Index (GCI) which accounts for changes in solution values, the order of discretization used and the local grid spacing [29]. To further minimise discretisation error, the present study employs an even smaller local grid spacing of 0.025m which leads to a global cell count of 9.4 million.

Airflow Simulation

Initial simulations used in the optimization study were all steady-state and isothermal and conducted using Fluent (Version 13.0Sp2). Further steady-state simulations were conducted at 2 and 12 ACH with heat sources on patient beds to explore the potential influence of thermal plumes. Double-precision real number representation was employed in conjunction with second order discretization for all governing flow equations

(i.e. mass, momentum and turbulence). Turbulence was simulated using the Reynolds Stress Model (RSM) which accounts for anisotropic turbulent structures in contrast to simpler Reynolds Averaged Navier-Stokes (RANS)-based models [30]. Previous studies have shown that the RSM model yields similar flow structures to the RANS k-e model for UV simulation [25] and better prediction of bioaerosol dispersion [31] in a mechanically ventilated room. Standard wall functions were employed giving solutions with average and maximum wall y^+ values of 15 and 38 respectively, for the 6ACH case. However, the focus of the study is on the bulk airflow and the flow in near-wall regions is far less important.

UVGI Modelling

UVGI performance depends on the irradiance field generated by UV lamps (E , W/m^2), the duration of exposure of a microorganism to the field (t , s) and the susceptibility of the microorganism to UV-C irradiance. The irradiance and exposure time are determined by the system design and airflow patterns. The product of these two variables defines the UV dose, D (J/m^2) received by airborne microorganisms, namely:

$$D(\bar{x}, t) = E(\bar{x})t \quad (1)$$

where \bar{x} is the position at time, t . The parameter D is cumulative and depends on the 3D UV field present within the space as well as the path taken by a given microorganism. For a known pathogen, the dose received by a microorganism can be used, together with the microorganism susceptibility [12], to calculate the expected microorganism survival fraction, and hence the reduction in airborne concentrations. For many hospital environments the actual pathogens present are unknown, so the dose is a good parameter to represent the effectiveness of a UVGI system without requiring knowledge of microorganism species.

The influence of the UVGI system is modelled here by evaluating the UV dose received by the air supplied to the ward, following the approach in Noakes *et al* [22]. While this method does not yield the same value of dose that would be delivered to a pathogen released by a patient [23], it is an approach that enables comparison of design scenarios when the infectious source location is not known. The method is implemented by treating the UV dose as a cumulative parameter; as air containing microorganisms passes through the UV field the dose received accumulates depending on the residence time and the irradiance. Considering equation (1), the rate of increase of dose in the UV field is given by:

$$\frac{dD(\bar{x}, t)}{dt} = E(\bar{x}) \quad (2)$$

Within the CFD model, the accumulation of UV dose is modelled using a non-diffusive passive scalar with equation (2) implemented as a source term. For a steady state scenario this yields

$$\nabla \cdot (\underline{UD}) + E(\bar{x}) = 0 \quad (3)$$

where the first term represents the distribution of dose by the velocity vector field, \underline{U} and the second term is the user defined source term. D is set to zero on the air inlet boundaries and accumulates with time depending on the local value of irradiance and the velocity field. The approach is comparable to calculating the age of air or residence time where a non-diffusive scalar can be used to calculate the age of a fluid using a source term of 1.0 s/s throughout a domain [32].

The UV field was based on that emitted from commercially available Lumalier WM236 wall mounted UVGI units (Lumalier Corporation, Memphis, Tennessee). It was assumed that there were three units in the ward each one located on either the windward or leeward wall of the ward, depending on the ward zone number. Each 0.92m wide UV unit has a series of stacked louvers that produce a 0.075m high collimated UV field. A previous investigation [19] included detailed radiometry measurements of the 3D irradiance field produced by this particular fixture. This field was then used in conjunction with CFD simulations of airflow in a small mechanically-ventilated room to predict the dose distribution using equation (3). Although the actual irradiance field was shown to vary in three dimensions with peak intensity occurring at the mid height of the collimated UV beam, previous simulations show that the device effectiveness can be accurately simulated using an equivalent 2D field (i.e. constant in the vertical direction) [19]. The 2D field is significantly easier to apply in a CFD model as the 3D field requires much greater vertical grid refinement in the vicinity of the lamps. For this reason the 2D field is employed throughout this investigation, with the planar UV field for each device stored as a fixed-value data set in the location of interest.

In order to model the effect of a UV device in multiple different locations, only the UV field was simulated and the physical device geometry was excluded from the model. This meant that multiple simulations could be run on the same mesh by simply redefining the UV field in a different location. To facilitate defining the UV field, the upper air region of the ward geometry was separated into single layers of cells, each 0.025m thick. For a particular device position, the resulting field was stored in three vertically-stacked layers of cells giving a total band thickness of 0.075m. Above and below this band the UV field is assumed to be zero. This is shown in Figure 2(a).

Figure 2(b) shows the resulting irradiance field in the horizontal plane with three co-planar fixtures active and located on the same wall. Taking the geometry of the space into consideration, it is logical to position each of the three devices above a bed and in between windows so that there is one fixture per zone, as shown in Figure 2(c). It is assumed that each fixture can be located at a minimum height from the floor of 2.185m up to a maximum of 2.810m in steps of 0.025m, giving 25 possible vertical positions. The minimum vertical location is based on the manufacturer recommended minimum mounting height for safety. Furthermore, each device can be located on either the windward or the leeward wall, extending the number of possible locations to 50 for each fixture. This can be controlled conveniently within the simulations using a single, normalized, location parameter, d_i , for the i^{th} zone. For $0.0 \leq d_i < 0.5$ the fixture is mounted within the

prescribed height range on the leeward wall, and for $0.5 \leq d_i \leq 1.0$, the fixtures are located on the windward wall, as shown in Figure 2(d).

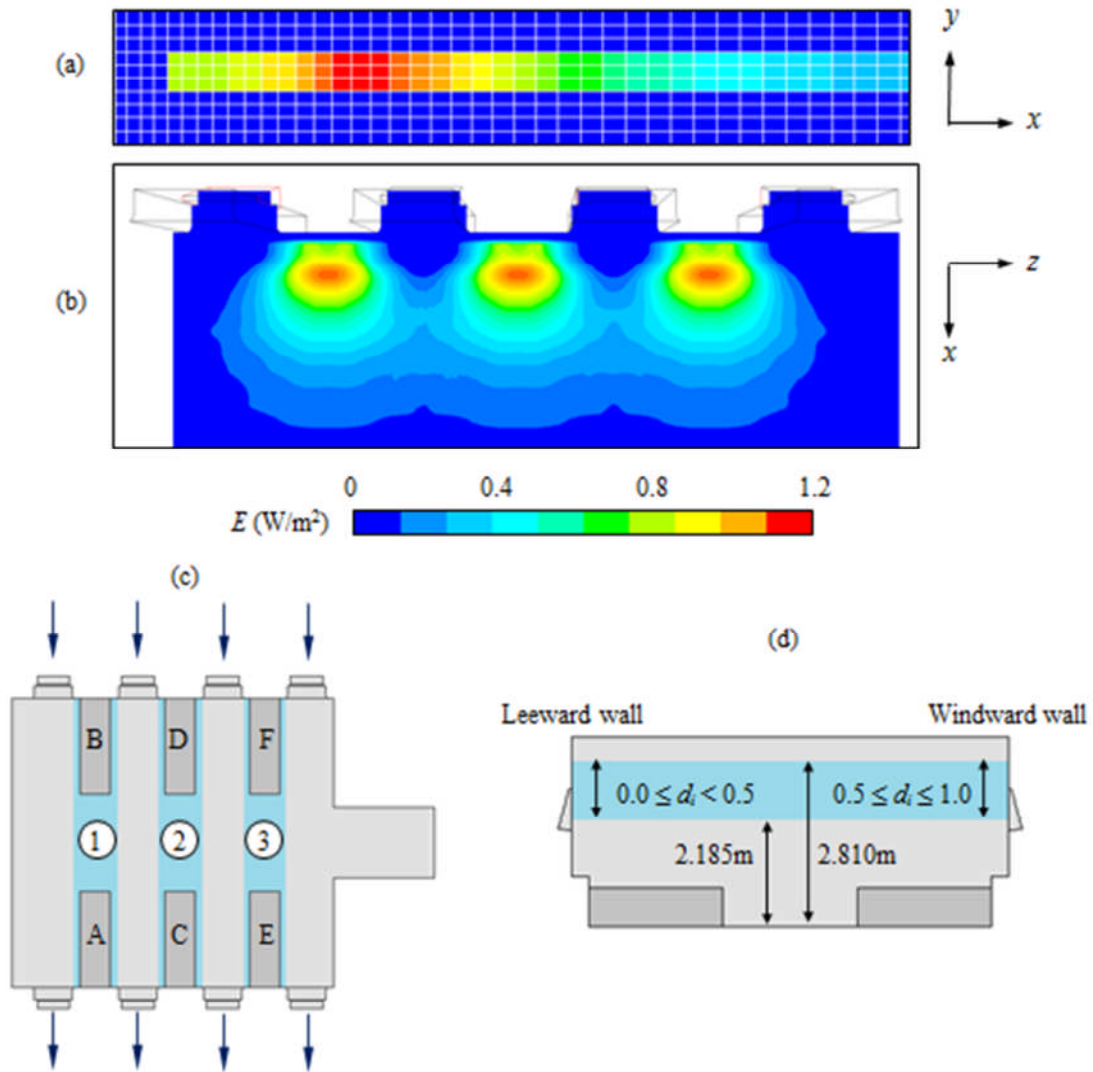


Figure. 2 (a) Vertical section through a UV device showing the local irradiance field and grid cells, (b) plan view of the irradiance field on a horizontal plane through the centre of three UV fixtures mounted on the windward wall of the hospital ward, (c) plan view of the whole ward with zones 1-3 and beds A-F labelled and (d) span-wise section through the ward showing the location parameter, d_i , and the possible locations for the i^{th} UV fixture.

Design of Experiments

As described above, the location of the three UV units is described through non-dimensional design parameters (d_1 , d_2 and d_3) and each one has 50 possible values. This results in a total of 125000 (50^3) potential combinations of the three UV fixtures. To conduct so many simulations would be prohibitive and so, for a given simulation budget, a Design of Experiments (DoE) can be used to select suitable combinations of design parameters. To do this, an Optimal Latin Hypercube (OLH) DoE [33] consisting of 50 points was chosen to evenly sample the design parameter space as shown in Figure 3. Here, each point represents a

unique combination of UV fixtures within the ward. To ensure an even spread of points within the design space, the Audze-Eglais potential energy optimality criterion is employed [34].

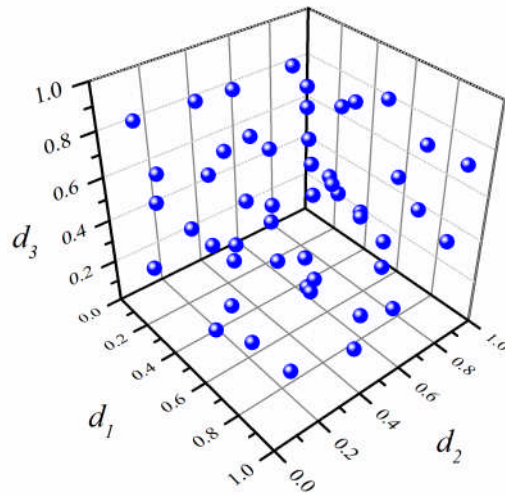


Figure 3. Design of Experiments (DoE) approach used to sample the design space to determine representative UV lamp configurations using the location parameter d_i .

Solution and Convergence

The simulations were run in parallel using a 64 core cluster consisting of 8 nodes each with 2 x dual-quad core 2.26 Ghz Nahalem processors and 24 Gb of SDD RAM. Converged airflow simulations at the three ventilation rates were first obtained before modelling the effect of the UV devices. The extra transport equations required by the RSM turbulence model initially led to convergence difficulties in the form of low-frequency oscillations. To remedy this, the solution was relaxed and the pressure-based solver (segregated) used for a total of 25000 iterations which significantly dampened the oscillations. This solution was subsequently used to initialize the second phase (also 25000 iterations) which required the density-based (coupled) solver, again in conjunction with lower under-relaxation factors. The strategy led to clear convergence in the form of flat residual levels of around $1e^{-5}$ for continuity and the turbulence equations and $1e^{-8}$ for the momentum equation. Dose simulations were then run for each of the 50 sample points (per ventilation rate) by solving the scalar transport equation (3) on the converged flow field. Scalar solution convergence was attained in approximately 200 iterations. Results from the simulations are presented throughout in terms of two parameters. D_W is the volume-averaged UV dose over the whole ward and is used as a single parameter to characterize the effectiveness of the UV devices over the whole space. D_{BED} is the average UV dose calculated in a $0.75 \times 0.70 \times 2.4$ m air volume directly above each bed, and was selected as a parameter representative of the patient breathing zone.

Numerical Optimisation

To demonstrate the potential of numerical optimisation, a problem was formulated as a means of determining the best combination of UV fixture locations for this particular Nightingale ward layout, for the 6ACH results only. Recent studies have demonstrated the feasibility of optimising indoor ventilation systems using numerical models [35,36] however, to the authors' knowledge, optimisation of the operation of passive UVGI systems has never been done before. Many different forms of numerical optimisation exist but metamodel-based techniques offer many benefits from an engineering stance [36,37]. As well as identifying the optimum design for a given system, metamodels also provide engineering insight because they typically require many data points by assessing multiple design variations. In the present study a moving least squares (MLS) [38,39] metamodeling approach is adopted because it allows for numerical noise which is prevalent in CFD responses [37,40,41]. The MLS approach requires CFD solutions (known as response values) for a range of designs so that an approximation can be built (the metamodel, also known as the response surface) and the best design found by searching the metamodel using formal numerical optimisation methods. The MLS differs from most commonly applied metamodeling techniques because it is based on approximations which allows for errors in the responses [37]. Other popular techniques such as kriging [42] utilize interpolations which go through the CFD responses and can be prone to 'over-fitting' and other undesirable behaviour [37]. In the present study a Gaussian weight decay function, w_i , is employed in conjunction with a closeness of fit parameter, θ , which is given by the following relation:

$$w_i = \exp(-\theta r_i^2) \quad (4)$$

where r_i is the Eclidean distance of the metamodel prediction location from the i^{th} point (i.e. each CFD response value). The metamodel can then be tuned using θ to give the best metamodel for the given application. This method has been verified in other engineering studies [36,37] and it is suitable for the present investigation. The purpose of the overall optimisation strategy (shown in Figure 4) is to identify UVGI fixture configurations which maximises the UV dose in (i) the whole ward (D_W) and (ii) in the vicinity of each bed, D_{BED} . Both D_W and D_{BED} are therefore the objective functions which are to be optimized, namely:

$$\max D(\mathbf{d}) \quad (5)$$

Where D is the dose quantity (i.e. D_W or D_{BED} depending on the objective function being optimised) and the vector \mathbf{d} denotes design variables d_1 , d_2 and d_3 which are the UVGI fixture location parameters defined in the earlier section. Note that the convention in numerical optimisation is to minimise objective functions and so the criteria used was to minimise the reciprocal of D_W and D_{BED} respectively, however, for clarity maximising dose represented by equation (5) and this is the terminology used for the remainder of this paper. Having defined the optimisation problem, the strategy shown below summarises the approach which consists of the

aforementioned DoE, the CFD responses, the MLS metamodel and the numerical optimization methodology. These are summarised in the following list and Figure 4..

1. Obtain D_W and D_{BED} from the CFD simulations for each of the 50 UVGI fixture configurations.
2. Construct MLS metamodels (one per objective function) using the dose data.
3. Use a combination of global (Genetic Algorithm, GA) and local (Sequential Quadratic Programming, SQP) optimisation techniques to search each metamodel for a candidate for the maximum dose.
4. Carry out a further CFD simulation on each candidate and update the metamodel.
5. Continue steps 3 and 4 iteratively until an optimum UVGI fixture configuration is converged upon for each metamodel.

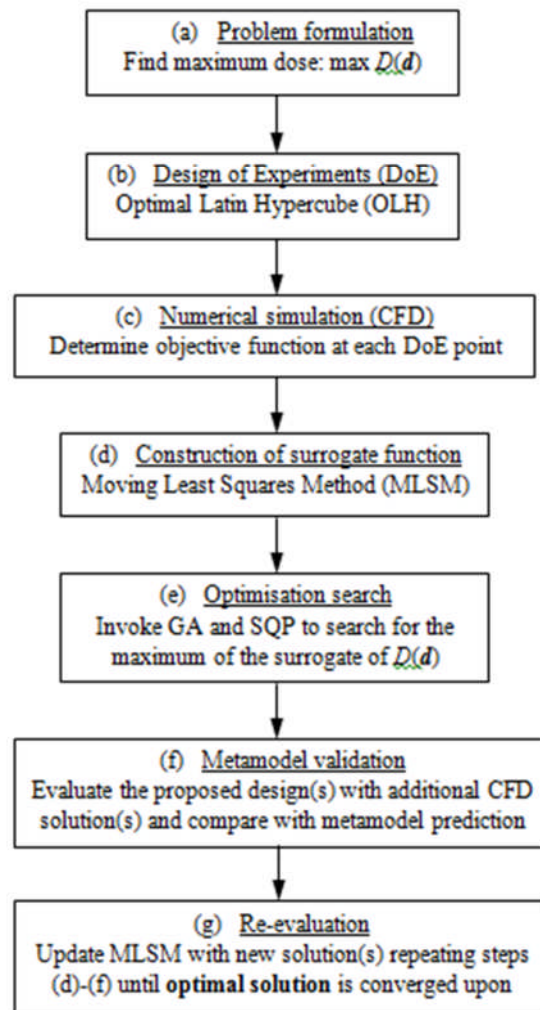


Figure 4. Flow chart showing the optimization strategy used to find the optimum UVGI fixture combination for maximising dose in the ward.

Results

Airflow Distribution

Figure 5 reveals the airflow structure produced by the cross-ventilation regime at 6 ACH. Figure 5(a) shows the incoming air enters the ward through the inlet windows and ceiling-level entrainment is evident. A proportion of the air passes straight across the ward and exits through the leeward windows whilst the remainder is forced downwards and turned back on itself before exiting, which serves to mix the airflow in the centre of the ward. Figure 5(b) shows contours of the velocity magnitude in a span-wise plane and another in the horizontal plane immediately below the top of the beds. As expected the air velocity in the lower region of the ward is slower because the casement style windows direct the incoming fresh air toward the ceiling (note the relatively high velocity jet projected at the ceiling). As the flow migrates across the ward, the high velocity air currents entrained on the ceiling reduce from 0.4 m/s to below 0.1 m/s before reaching the leeward side of the building. While quantitative comparison was not available, this airflow pattern concurs with that seen experimentally using a smoke tracer in an unoccupied Nightingale ward [25]. This flow visualization is shown in Figure 6 which illustrates the flow structure near opposing inlet and outlet windows. The inlet flow follows the angle of the casement-style window opening (Figure 6(a)) while the outlet flows (Figure 6(b)-(d)) highlight the span-wise tendency of the mean flow current as the tracer is directed towards the lower, open part of the window.

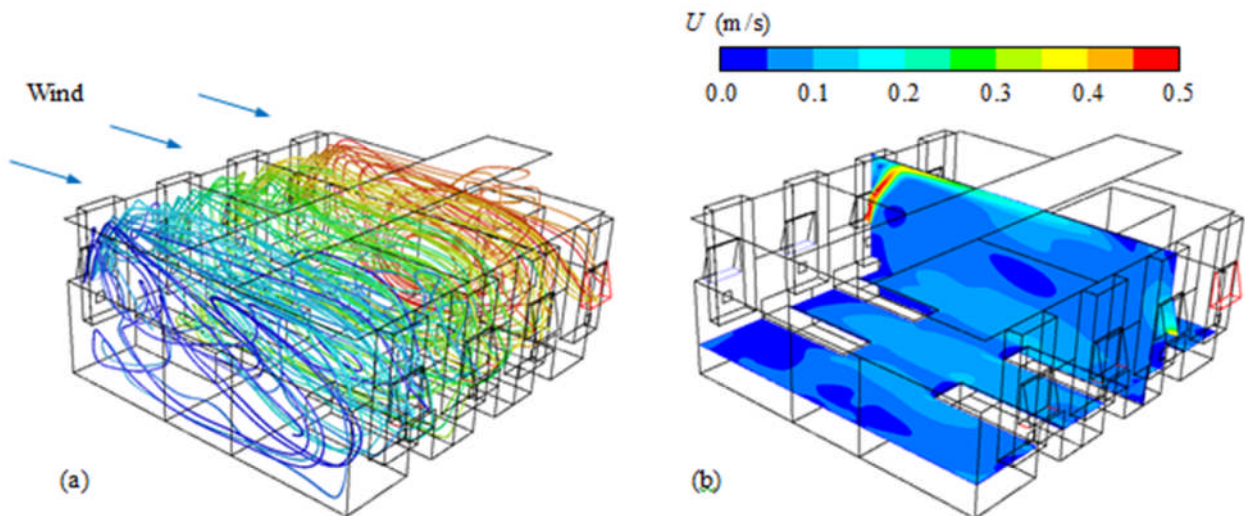


Figure 5. Airflow characteristics at 6 ACH (a) Pathlines generated from the left-to-right cross-ventilation regime and (b) contour plots of the velocity magnitude, U , in a span-wise plane and another at bed level.

Pathlines coloured by particle identity (not flow variables) for clarity.

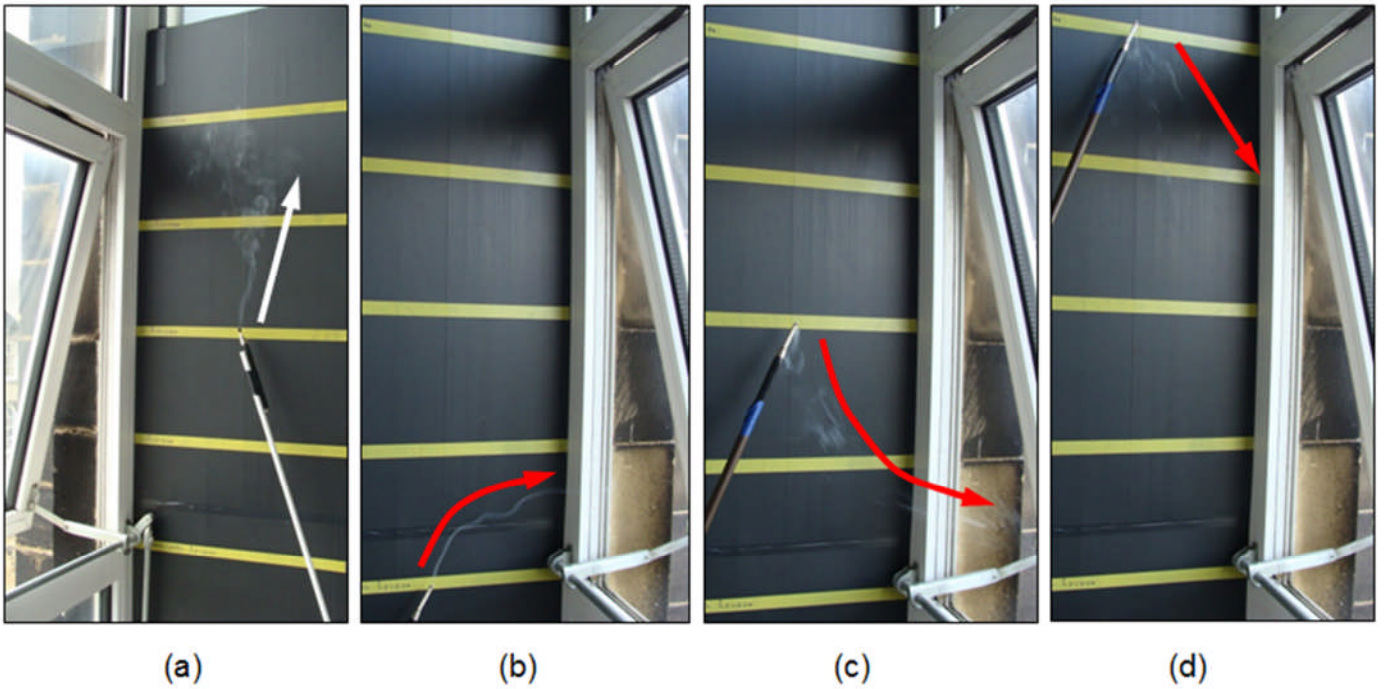


Figure 6. Experimental flow visualization via smoke sticks showing the flow structure near (a) one inlet window and (b)-(d) an opposing outlet window at three heights, each separated by 0.4 m vertically.

Figure 7(a) and (b) show velocity profiles for the 6 ACH case at heights of 1.0 m, 1.5 m and 2.0 m on a span-wise section through the ward along the centreline of beds C to D (see Figure 2(b)). Note that the prevailing wind direction is effectively from left to right as the windward window begins at $x = 0$ with the leeward window at $x = 7.2$ m. The lowest profile ($y = 1.0$ m) shows that the velocity magnitude of the airflow, U , is small above the windward bed (bed D) whereas the opposing leeward bed (bed C) experiences a far greater velocity. This is because the angle of entry of the incoming air is directed toward the ceiling (i.e. away from bed D) where the flow entrains before crossing to the leeward side of the ward before flowing down towards bed C. The resulting recirculation pattern effectively supplies the leeward bed with the greater air velocities. This flow pattern is indicated by the elevated air velocities being skewed toward the leeward side of the ward for the highest profile ($y = 2.0$ m) both in terms of the velocity magnitude (Figure 7(a)) and the span-wise velocity, U_x , (Figure 7(b)). The recirculation is particularly evident from the span-wise air velocities where the highest profile has a largely windward direction, whereas the lower profiles ($y = 1.0$ m and 1.5 m) are dominated by leeward airflow currents as the flow has turned back on itself, see Figure 6(b). Figure 7(c) shows a comparison of the span-wise velocity normalised in terms of the inlet velocity magnitude, U_{IN} , for all three ventilation rates (i.e. 2, 6 and 12 ACH) at the intermediate height of $y = 1.5$ m. This shows that all three flow patterns are fundamentally very similar and this was observed at the other two heights (though not shown here).

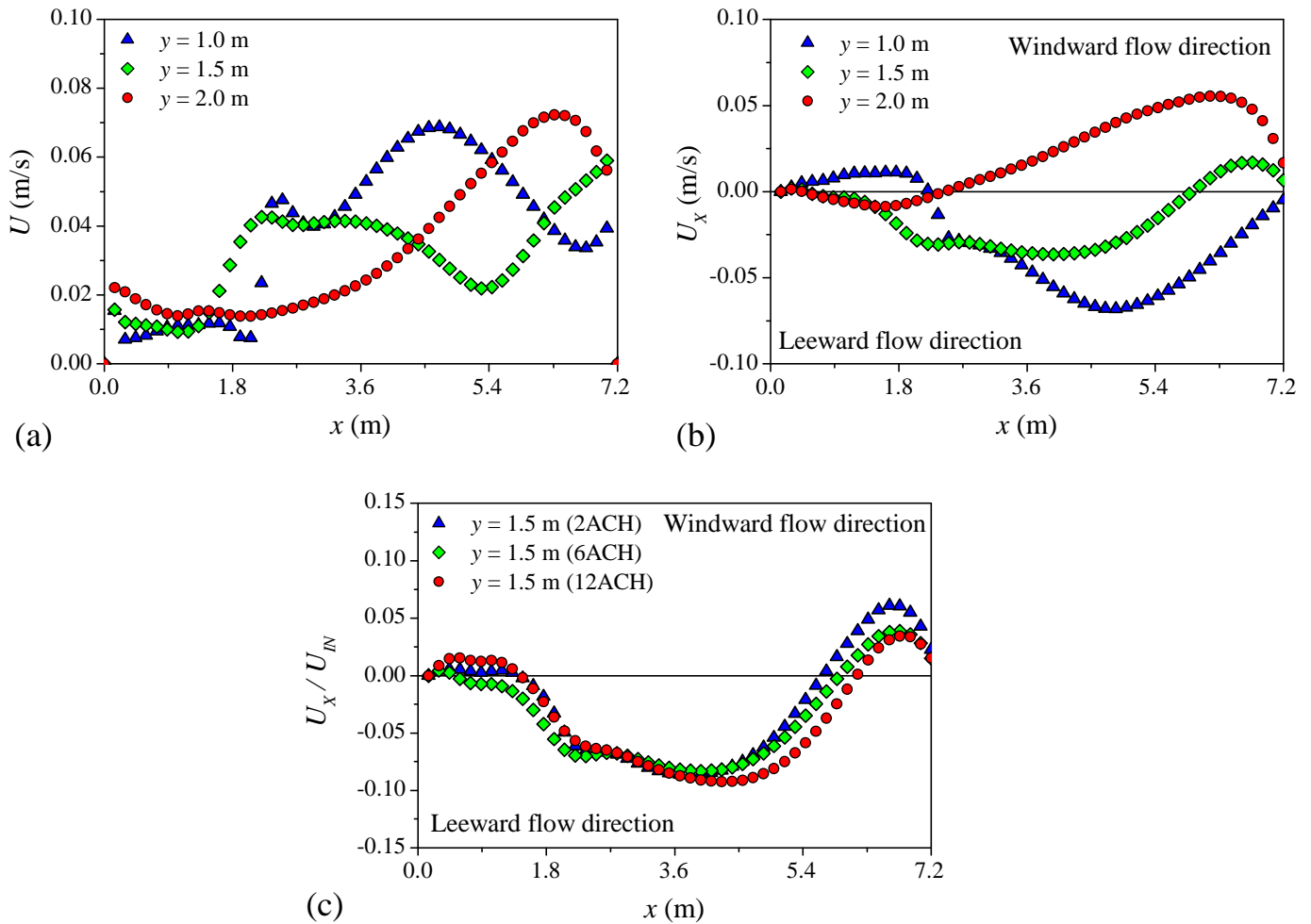


Figure 7. Span-wise velocity profiles along lines connecting the centreline of beds C and D. (a) Velocity magnitude at 6ACH at three heights, (b) x-component of velocity at 6ACH at three heights, (c) normalized x-component of velocity at ventilation rates of 2,6 and 12 ACH at a height of 1.5m. Note the windward side of the ward is on the left of the plot with cross-ventilation from left to right.

Dose Distribution

Figure 8 shows contour plots of the dose (J/m^2) in the vertical direction for a ventilation rate of 6 ACH, whereby fixtures in zones 1 and 2 are mounted on the leeward wall with the zone 3 fixture located on the windward wall. As expected, the dose increases immediately in front of each fixture where the UV irradiance is highest; this effect is most noticeable in front of the zone 3 fixture mounted on the windward wall. For the fixtures to be effective however, the dose must be distributed throughout the room as this indicates that air passing through the UV field has been disinfected to some extent and is re-entering the occupied space with lower infection potential. Both leeward fixtures (zones 1 and 2) are effective at increasing the dose in the lower patient level, which occurs by virtue of the greater mixing present. The incoming fresh air passes through the high-intensity UV field and returns back towards the windward side. For the windward mounted fixture the dose level is higher in its immediate vicinity (white region), however some of this air exits the ward without further mixing and a lower dose is evident in the patient zone, particularly on the leeward side of the ward.

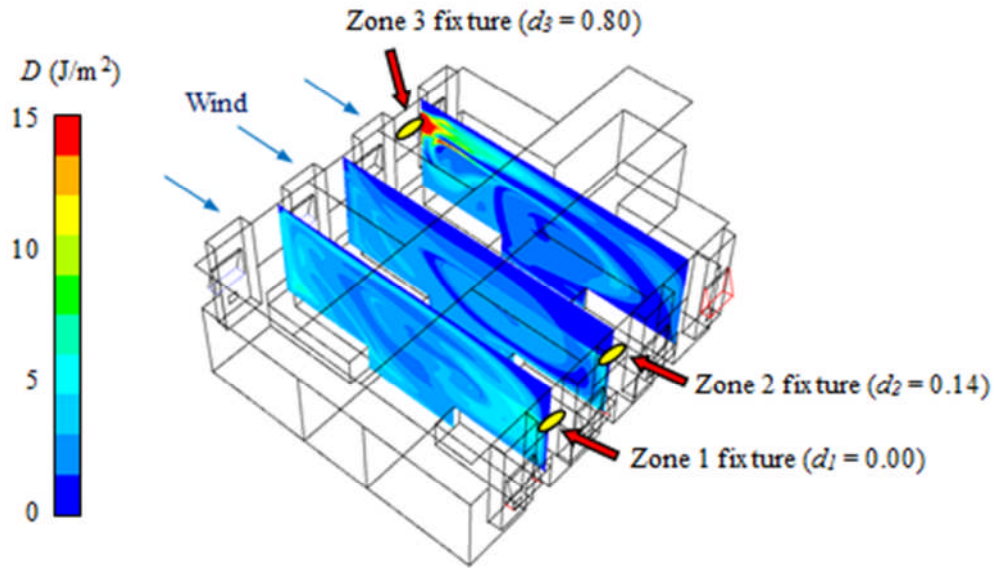


Figure. 8 Contour plot of the dose distribution at 6 ACH resulting from one combination of UV fixtures with two mounted on the leeward wall (zones 1 and 2) and the remaining one on the windward side (zone 3).

To assess the performance of the UVGI fixtures within the ward, results from the 50 combinations (per ventilation rate) are compared against each other. As discussed, two parameters are of interest. Firstly the volume-averaged ward dose, D_W , considers how the dose varies as a function of the location parameter per fixture (i.e. d_1 , d_2 and d_3) at a whole ward level. Secondly, D_{BED} , represents the average dose at bed level over the whole ward and is used to consider the impact of the fixtures at the patient locations. Figure 9 considers the ward and bed average dose at a ventilation rate of 6 ACH. Each point represents a particular set of fixture combinations and the same data is presented in three separate plots to explore the influence of each fixture location. In all cases the three UV devices are treated as a system to treat the whole ward and the focus is on influence of positioning on the system level performance; as dose is a parameter that is transported by the airflow it cannot be assumed that the dose in a particular zone is only influenced by the lamp in that zone. The three fixtures lead to a ward level dose in the range $D_W = 1.04 \text{ J/m}^2$ to $D_W = 1.63 \text{ J/m}^2$, while bed level dose is more variable with a range $D_{BED} = 0.97 \text{ J/m}^2$ to $D_{BED} = 1.93 \text{ J/m}^2$. Whilst there is a good deal of scatter in the data the results do suggest that some fixture positions lead to better results than others. For the leeward fixture positions ($0.0 \leq d_i < 0.5$), the dose is generally higher when the fixture is mounted at the lower end of the prescribed height range (i.e. d_i is close to 0.0). This trend is particularly noticeable in zone 2 where the dose decreases with increasing fixture height; at the ward and bed level the lowest doses occur with the zone 2 leeward fixture mounted high, see Figure 9(c). For the windward fixtures ($0.5 \leq d_i \leq 1.0$) there is no clear relationship with fixture location and significant scatter in the data is evident in these cases, Figures 9(b), (d) and (f).

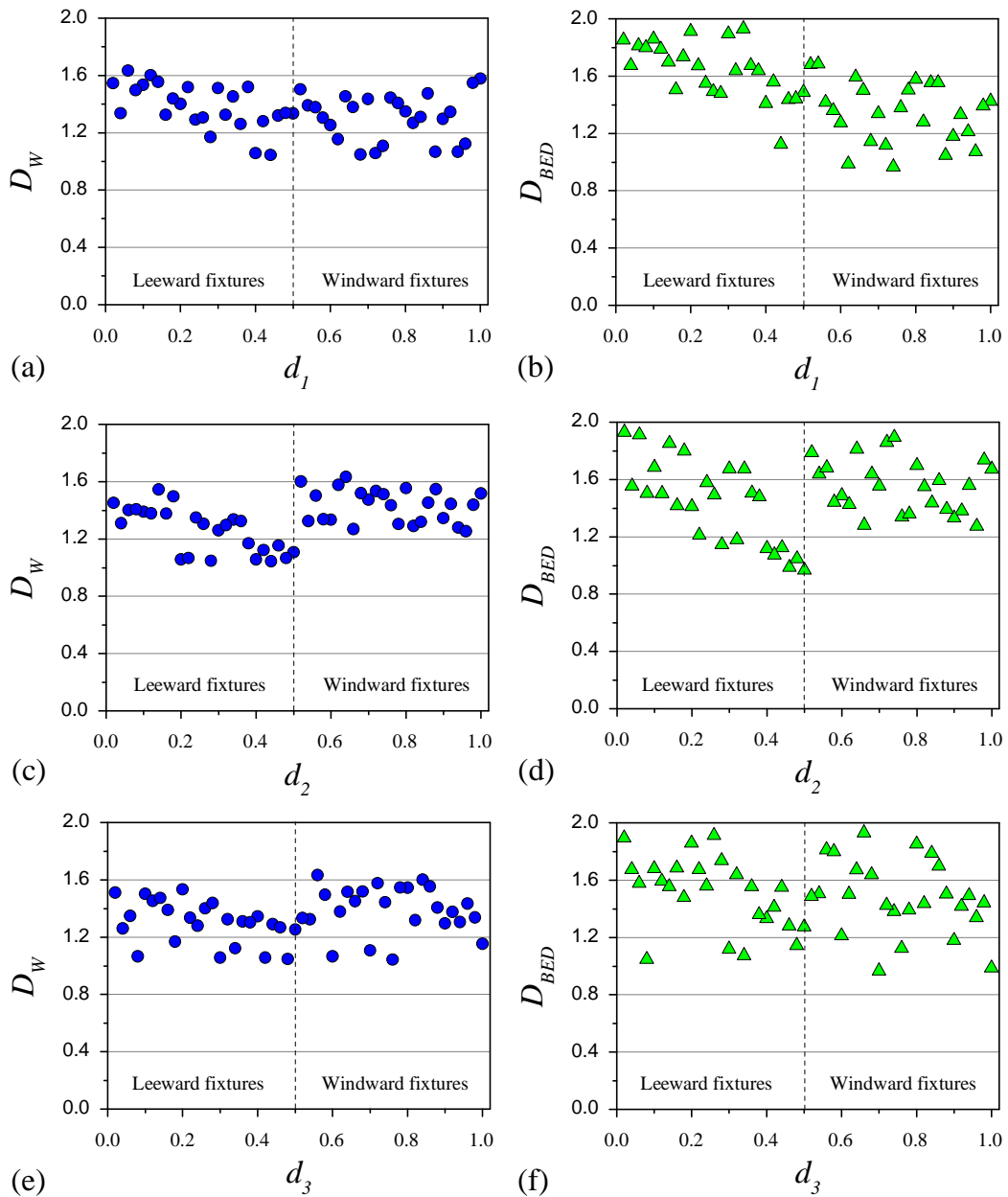


Figure. 9 Relationship between the UV fixture position parameters (d_1 , d_2 and d_3) and the ward-averaged (D_W) and bed-average (D_{BED}) dose in the ward, at a ventilation rate of 6 ACH.

Figure 10 shows bed-level dose values only, for the three fixture zones at ventilation rates of 2 and 12 ACH. As expected, dose values at 2 ACH are higher ($2.35 \text{ J/m}^2 < D_{BED} < 6.13 \text{ J/m}^2$) than those seen at 6 ACH, while dose values at 12 ACH are lower ($0.47 \text{ J/m}^2 < D_{BED} < 0.99 \text{ J/m}^2$). In both cases there is a noticeable dependence on the location of the central fixture position, d_2 , which is extremely prominent in the results at 2 ACH, see Figure 10(c). Here the dose values seen with the central fixture located in a leeward position are substantially lower with a marked decrease with increasing height compared to location on the windward side of the ward. This trend highlights the importance of the position of the central fixture which is apparent at all three air change rates and suggests that this fixture may be the most sensitive to airflow patterns within the ward.

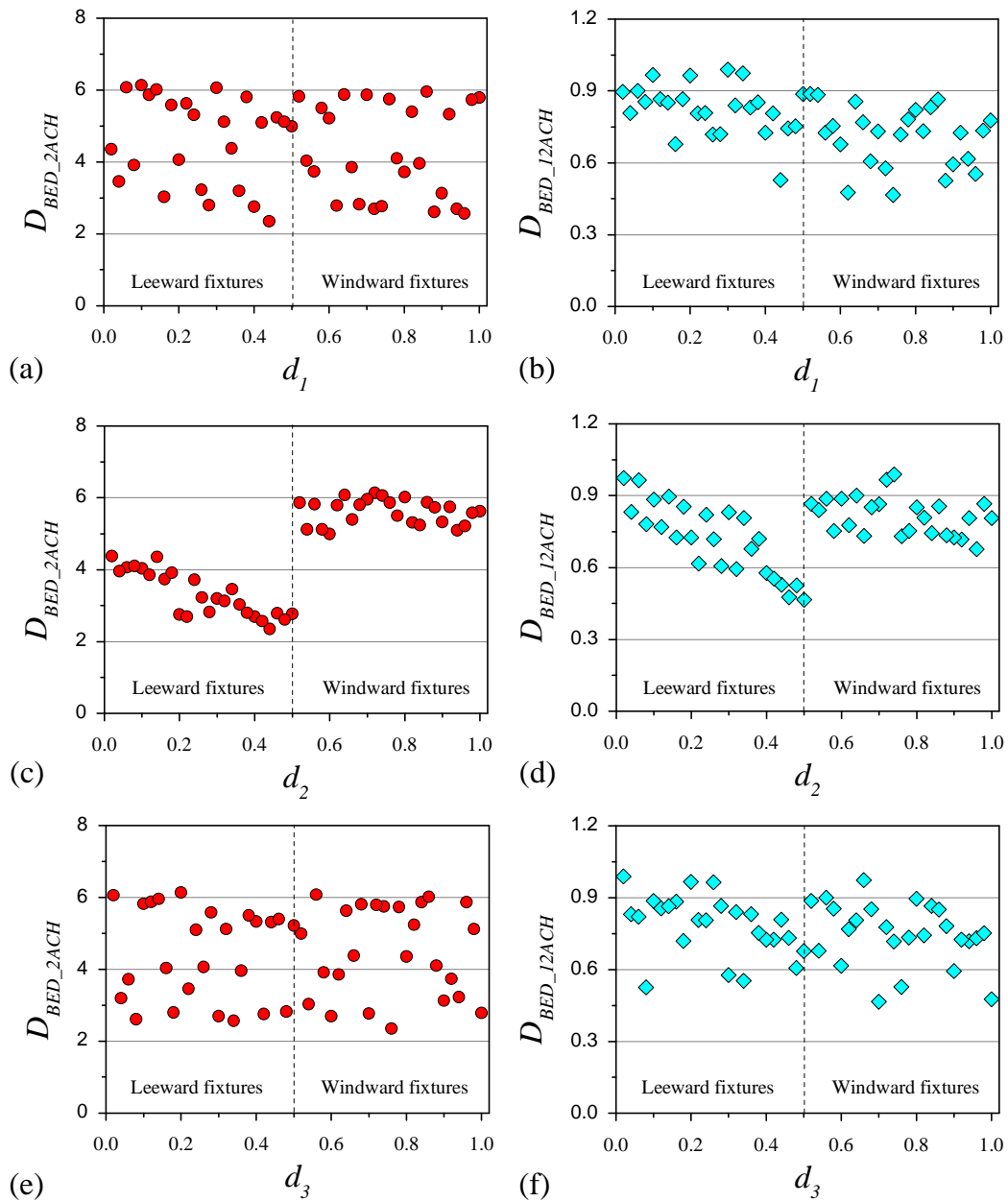


Figure 10. Relationship between the UV fixture position parameters (d_1 , d_2 and d_3) and the bed-average dose at a ventilation rate of 2 ACH (D_{BED_2ACH}) and 12 ACH (D_{BED_12ACH}).

Variability in dose distribution is also considered in Figure 11, which indicates how the average dose varies at each bed depending on the UV fixture combination from the 50 studied. In each case the results are plotted as the mean dose at each bed for all simulations with the error bars representing one standard deviation. As seen in Figures 9 and 10, the results in Figure 11 also demonstrate the greater variability in simulated dose at the lower ventilation rate of 2 ACH, where ward-air mixing is less prevalent. It is also noticeable that the bed experiencing both the highest average dose and the greatest range is that located centrally on the windward side of the ward (bed D) in fixture zone 2.

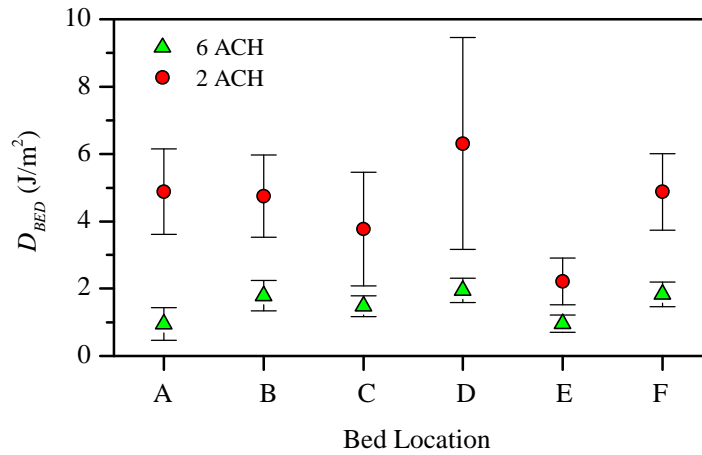


Figure 11. Variability in local bed dose at a ventilation rate of 2 and 6 ACH

Optimisation results

While the results in Figures 9 and 10 demonstrate the potential dose range achievable under different ventilation rates, it is difficult to draw firm conclusions about the best combination of fixture locations. In order to explore this further, the numerical optimisation strategy discussed in section 2.6 was applied to the data set at 6 ACH, using the commercial optimisation package Hyperstudy (version 11). Initial metamodels of (i) the ward dose, D_W , and (ii) the bed-average dose, D_{BED} were constructed using the data from each of the 50 UVGI fixture combinations. Global optimisation on the metamodels was done using a genetic algorithm (GA) followed by local optimisation via the sequential quadratic programming (SQP) technique, the latter ensuring that the optimum had been located by the GA on the metamodel. A candidate for maximum dose was identified for each metamodel and the corresponding UVGI fixture layouts assessed with new CFD simulations. Metamodel rebuilding with the additional CFD responses for dose did not yield an optimum result in the first iteration. The process was repeated (as per steps 3 and 4 in section 2.6) until optimum results were found for both objective functions (i.e. D_W and D_{BED}). In total this required a further 12 CFD simulations and the results are shown in Figure 12. It should be noted that 50 initial designs were used via the DoE to train the initial metamodel prior to optimization. This number is a practical balance between having sufficient data without requiring a prohibitively large number of simulations. Given that there are three design variables, d , the total number of initial simulations run was $16.7d$ which corresponds to another recent design optimization study [37] This number is significantly more than the general recommendation of $10d$ suggested by Loeppky *et al* [43].

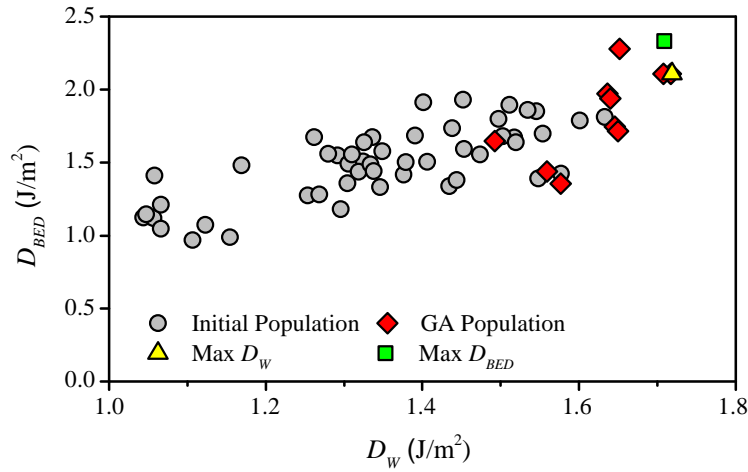


Figure 12. Objective function plot showing the initial population of 50 UVGI fixture combinations, the GA search population and optimum results for D_W and D_{BED} .

In terms of ward dose the optimum lamp configuration (max D_W) offered an improvement of 5.3% compared to the best design from the initial population of 50 fixture configurations. For optimum bed dose (max D_{BED}) the corresponding improvement was 20.8% which illustrates the potential of numerical optimisation in this context. Note that all results shown in Figure 10 are from actual CFD solutions i.e. optimisation predictions are validated. Both optimum designs exist in corner points of the design space with the only parameter distinguishing them being the position of the central fixture which is governed by d_2 , see Table 2.

Configuration	d_1	d_2	d_3	D_W J/m ²	D_{BED} J/m ²
Max D_W	0.0	1.0	0.0	1.719	2.108
Max D_{BED}	0.0	0.0	0.0	1.709	2.331

Table 2. Results from the numerical optimisation

This result shows that the best lamp configuration for maximising the bed-average dose is to have all three fixtures mounted at the lowest permissible height of 2.185 m on the leeward wall. Referring back to Figure 8, the zone 1 fixture is also located at this height in the leeward wall and the increase in dose in the lower extremities of the ward is evident. Clearly this mounting position combined with the natural ventilation regime within this particular ward leads to the best disinfection potential. In order to maximise the dose in the ward as a whole, the only difference is to have the central fixture mounted on the windward wall but again the height should be at the minimum permissible level (as above) to ensure close interaction with the patients. This underlines the earlier observation that the central fixture is extremely sensitive to the dose levels observed in the ward. Based on the results presented in table 2, the overall optimum for design purposes, under this flow regime, would be to mount all three fixtures on the leeward wall, 2.185 m above the ground. Such a configuration gives the largest overall bed-average dose and the corresponding ward dose is only 0.56% less than that for the maximum ward-level dose fixture configuration.

Thermal Effects

While the results above illustrate that the UV dose and airflow interaction can be modelled and an optimization approach applied, the airflows are based on a previous experimental scenario and do not include heat sources. To gain an initial understanding of the influence of heat sources on the flow, additional simulations were conducted at 2 and 12 ACH with a constant temperature of 35 degrees C applied on the surface of each of the patient beds to represent the patient heat load. Simulations were conducted for the optimum configuration determined, i.e. all UV fixtures on the leeward wall at the minimum permissible level. Figure 13 shows the influence of the heat sources on the dose distribution at 2 ACH. It can be seen that the thermal plumes change the flow pattern, creating two contra-rotating recirculation zones (see Figure 13(b)) and reducing the effectiveness of the cross ventilation flow which is evident in the isothermal case (Figure 13(a)). At 12 ACH the influence is less apparent; cross-ventilation still dominates the flow, although the addition of heat sources acts to increase the concentration of UV dose at the centre of the room. As shown in Table 3 the overall impact of heat sources on ward level dose is small at 12 ACH with a reduction of only 0.7%, but significant at 2ACH, with predicted dose substantially lower showing a 36.6% reduction. An important point to note is that these results are specifically for the optimum configuration found previously, however, this may change with ventilation rate and the degree of additional heat load.

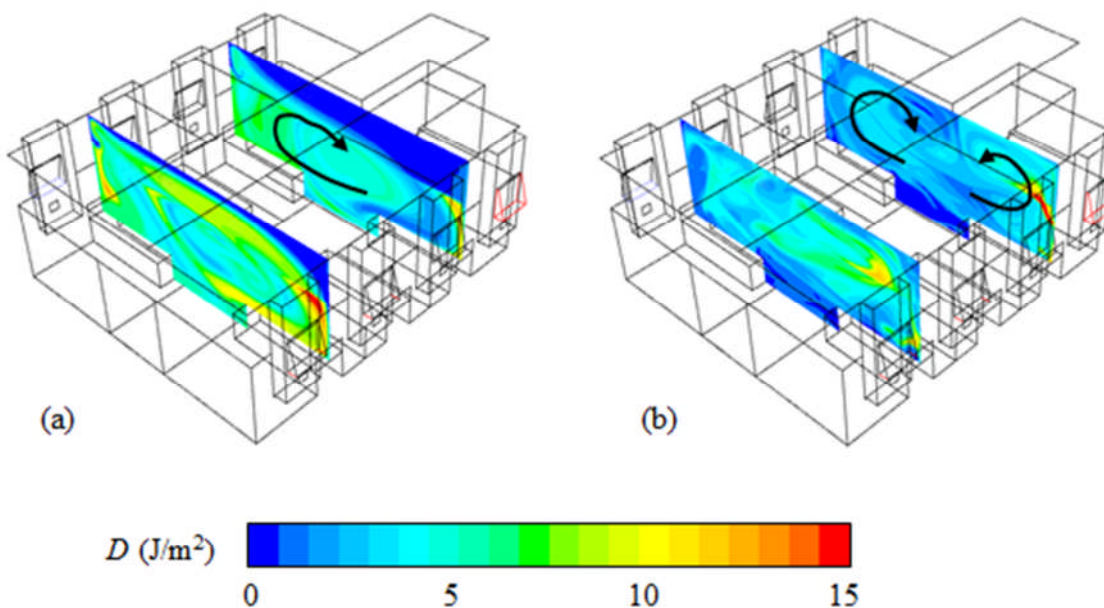


Figure 13. Contour plots showing dose distribution at 2 ACH for (a) isothermal and (b) thermal cases.

Ventilation rate (ACH)	Isothermal		Thermal	
	D_W J/m ²	D_{BED} J/m ²	D_W J/m ²	D_{BED} J/m ²
2	4.296	5.2836	2.725	2.038
12	0.888	1.157	0.882	0.7854

Table 3: Influence of heat sources on ward and bed dose with UV devices on the leeward wall at the minimum height

Discussion

Overall, the results show that the dose experienced in the ward is sensitive to both the UV fixture configuration and the ventilation rate and that the modelling approach allows this interaction to be evaluated. The results also show that heat sources may be an important factor in the air distribution, particularly at low ventilation rates. In modelling UV systems and applying to a real setting a number of aspects are important, which are discussed below.

Modelling Considerations

The results presented here indicate that by modelling the interactions between a cross-ventilation flow and a UVGI system it is possible to gain insight into how such devices are likely perform in naturally ventilated environments. However, the findings are based on a CFD modelling approach which is a simplification of reality and does have limitations. Full validation of the model was not possible. While comparison of actual UVGI performance with CFD models is possible for laboratory rigs [16] and small mechanically ventilated bioaerosol chambers [20], microorganisms cannot be released safely in a real environment to measure performance. However some validation of aspects of the model was carried out. Experimental data was used in defining the UV field [19] to ensure that this was a realistic representation of the fixtures. The isothermal airflow simulations were set up to replicate conditions in experimental assessments of airflows in a real but disused hospital ward [25]. Smoke tracer confirmed that windows acted as inlets and outlets under normal wind conditions and that air inlet followed the window angle [25]. This together with measurements of the ventilation rates were used to inform the airflow boundary conditions [28]. The model does have limitations with respect to thermal conditions and transient behaviour. As the experiments did not include the thermal sources present due to people and equipment in real hospital wards, isothermal conditions were assumed in the initial model and the resulting simulated airflow patterns are qualitatively similar to those observed in smoke tracer experiments conducted in the real ward [25], giving confidence in the airflow model. Addition of heat sources in the later simulations illustrate that thermal effects will have an influence in reality and they are likely to alter flow patterns particularly at low ventilation rates, where upward velocities due to heat sources are comparable to those induced by wind conditions. The findings suggest that these thermal plumes may reduce the mixing in the ward and hence the UV effectiveness; in such cases the addition of mixing fans as recommended by Zhu et al [24] may be beneficial. In a real scenario there will also be some heat

generation due to the UV devices, which will also have an impact on the flow. However this is likely to be small compared to the thermal effects of people and heating systems. The simulations are based on Lumalier fixtures with a manufacturer stated electrical power consumption of 72W and a UV output of 24W. The difference between these two values (48W) will be emitted as heat and visible light, and as such the heat generation is comparable to many conventional visible light fixtures. Similarly movement of people in a real environment will also alter the flow patterns. Simulating this realistically in a CFD study presents a significant challenge, however it is possible that movement will lead to increased air mixing in the ward, which has been shown to be beneficial for the performance of upper room UV [24]. The results also only apply to steady state cross ventilation wind conditions. In naturally ventilated spaces the flow patterns seen in reality are driven by the fluctuating external conditions and can be very different from one moment to the next.

In addition to the airflow modelling, the study demonstrates that numerical optimisation can be used to determine the best UVGI fixture combination. As the fixture parameter design space is three dimensional (Figure 3) it is not possible to view how these influence the objective functions in one single plot. Figures 9-11 were useful in identifying trends, however, the use of metamodels was essential in determining optimum fixture combinations. Both objective functions were optimised with an additional 12 UVGI fixture assessments required to achieve this. The results are perfectly logical which demonstrates that the metamodel-based optimization employed successfully captured the flow physics; this is a direct result of the initial population of fifty UVGI fixture assessments which effectively trained the metamodel. Although the optimum results are logical and sensible, this was not apparent from the outset and this highlights the potential for numerical optimisation to aid hospital ward design.

Infection Control Implications

The CFD study carried out here focused on modelling the dose distribution, a parameter that depends on physical attributes (the UV field and the airflow patterns) but has no dependence on any infectious agents present. The dose required to inactivate a given microorganism depends on its susceptibility, which in turn depends on species, strain and environmental factors such the temperature and humidity [14,15]. The relationship between airborne microorganism concentration, $C(t)$ and UV dose can be represented using an appropriate decay model. In many cases a first-order decay is a suitable approximation and is given by:

$$\frac{C(t)}{C_o} = e^{-kD} \quad (6)$$

Here C_o represents the initial microorganism concentration and the term, k (m^2/J), represents the microorganism susceptibility constant [12]. Microorganism susceptibilities are determined experimentally, and published values can vary substantially, which may be due to the experimental conditions or the

particular strain of microorganism used. However, such values are necessary to determine the potential risk reduction that may be achieved through installation of UVGI devices.

In order to evaluate the potential benefits that may be achieved through the system considered in this study both dose and inactivation are considered in a comparable mixing ventilation model. Such ventilation models have been applied to evaluating upper room UV performance in a laboratory setting [15, 44]. The model is derived by assuming a room volume of 200 m³, a ceiling height of 3.5 m and treating the upper 1m of the room as a UV zone. Dose can be determined from equation (1) with the irradiance, E , taken as an average value over the upper zone of the room and the residence time of the air in the UV zone calculated from V_{uv}/Q , where V_{uv} is the volume of the upper zone and Q is the room ventilation rate (m³/s). The upper zone irradiance was calculated from the plane average irradiance from the CFD model with all three devices located on the same plane, $E_p = 0.12$ W/m²; this in turn is derived from experimental measurements [19]. For a given constant generation rate of infectious particles, q (cfu/s), the resulting steady-state airborne concentration, C (cfu/m³), can be calculated by considering the removal due to UV disinfection and the removal due to ventilation dilution [15] as:

$$C = \frac{q}{Q(1+kD)} \quad (7)$$

The microorganism susceptibility constant was assumed as $k = 0.4$ m²/J, a value representative of TB (NIOSH [45] indicate susceptibilities in the range 0.23-0.55 m²/J). Table 4 presents the dose calculated by this mixing model alongside the average ward level dose based on all the CFD simulations. It can be seen that the average dose from the mixing model is slightly higher than the CFD average, but is a comparable value. This is as expected as the mixing model assumes ideal conditions that are not present in the CFD simulation. Table 4 also shows the percentage reduction in airborne microorganisms that may be expected due to the UV devices alone for each air change rate, and the total reduction due to ventilation alone and UV and ventilation combined with respect to the expected concentration at 2ACH without a UVGI system. As expected, the relative efficacy of the UV system depends on the ventilation rate with an expected reduction due to UV of around 65% at 2 ACH reducing to 23% at 12 ACH. However, in considering system performance it is the total risk reduction due to the combined effect of UV and ventilation that is significant. While the reduction in risk at 6 and 12 ACH is dominated by the ventilation flow, the installation of a UV system at 2ACH results in a total reduction only marginally below what could be expected by ventilation alone at 6 ACH.

Ventilation rate (ACH)	D_w Mixing model	D_w CFD Average	Airborne reduction due to UV (%)	Reduction due to ventilation w.r.t 2 ACH (%)	Total reduction w.r.t 2 ACH (%)
2	4.629	4.06	64.9	0	64.9
6	1.543	1.35	38.2	66.7	79.4
12	0.771	0.727	23.6	83.3	87.3

Table 4: Comparison of CFD predictions with mixing ventilation model

Design Issues

The study presented here considered installation of three wall mounted devices in a relatively large space. The model was constrained by practical aspects to some extent in that we identified six realistic wall locations where fixtures could be mounted. Although the results indicate that the best configurations tend to be achieved with the fixtures mounted at the lowest mounting height, the practical and safety aspects to this would have to be considered in any design; the irradiance field produced by UVGI fixtures is harmful to the occupants if they are directly exposed. Manufacturers generally recommend minimum mounting heights of at least 2m to overcome safety issues and hence in reality fixtures may have to be mounted higher to overcome any risks. The results also focused on two parameters, the overall average dose D_W and the dose in patient zones D_{BED} . While the results were largely consistent between these two parameters suggesting they are representative of effectiveness, there are other parameters that may be of more relevance in some cases. For example, if a UV installation is design to protect healthcare workers from patients with respiratory infections basing design decisions on the maximum dose at healthcare worker breathing height may be a more appropriate measure.

The results presented will of course depend on the particular pathogen concerned and other factors such as the location of the source and susceptible patients, however they do suggest that upper-room UV could be beneficial in naturally ventilated wards. In particular there could be good benefits from operating a UVGI system when the conditions are such that the wind-driven ventilation rate is low, providing there is a sufficient level of mixing in the ward. It is also worth commenting that the installed planar UV field in this model (around 0.12 W/m^2) is below that recommended by NIOSH [45] who suggest a plane average irradiance of $0.3\text{-}0.5 \text{ W/m}^2$. Increasing the fixture output to achieve this level would further increase any benefits; this could be achieved through installing extra fixtures or fixtures with a higher output.

Installation of a UVGI system may also be an energy efficient solution to improving infection control, particularly in climates where increased ventilation may lead to high heat losses or gains. As shown in Table 2, at low ventilation rates installation of a UV system may be able to produce an improvement in microbial air quality comparable to doubling or tripling the ventilation rate. Energy data on UV systems is limited, but a small number of studies have carried out calculations to explore benefits. Ko et al [8] consider the effectiveness of UV against TB transmission in a waiting room and calculate that UV may be less expensive than increased ventilation by between 3 and 13 times [46]. We recently conducted a modelling study [9] that suggested that installation of UV can achieve reductions in airborne risk comparable to or better than increasing the ventilation rate from 3 to 6 ACH at 11-55% of the energy cost, depending on the scenario. These studies suggest that the energy requirement may well be considerably lower than increasing ventilation rates.

Conclusions

A numerical study of natural cross-ventilation applied to a six-bed Nightingale ward was conducted. A series of simulations were carried out to investigate how the placement of upper-room UV disinfection fixtures influences the air disinfection potential. Results show that both the fixture height and choice of wall to mount each one have a marked effect on the performance under isothermal conditions. While all installations will be beneficial, mounting the fixtures at low levels on the leeward side of the ward appears to yield the best coverage as it allows for close interaction between patients and disinfected air currents which emanate from the front of the UVGI fixtures. However, the results are specific to the ward layout and the ventilation rate and regime studied. In particular, initial simulations carried out with patient heat sources included indicate that thermal effects may be significant at low ventilation rates, reducing mixing and hence UV effectiveness. This influence will be case specific, depending on the ventilation flow and location of heat sources in a particular environment. Application of the numerical optimisation approach at 6 ACH is successful and demonstrates how this approach can be used for selection of the best design location for the UV devices. Work is on-going to apply numerical optimisation to a range of ventilation rates to identify optimum design configurations which are effective across a range of conditions.

Acknowledgments

The authors would like to thank the UK Engineering and Physical Sciences Research Council (EPSRC) for funding this research and to the estates staff of Bradford NHS Foundation Trust for their collaboration.

Dr C.J. Noakes was the lead investigator, Dr C.A. Gilkeson conducted the CFD modelling and analysis of results, Dr M.A.I Khan contributed to the optimization study, all authors contributed to the preparation of the manuscript. The authors have no conflicts of interest to declare.

References

1. Eames I, Tang JW, Li Y and Wilson P. Airborne transmission of disease in hospitals. *Journal of the Royal Society Interface* 2009; 6: S697-S702.
2. Nielsen PV. Control of airborne infectious diseases. *Journal of the Royal Society Interface* 2009; 6: S747-S755.
3. Gustafson TL, Lavelly GB, Brawner ER Jr, Hutcheson RH Jr, Wright PF and Schaffner W. An Outbreak of Airborne Nosocomial Varicella. *Pediatrics* 1982;70;550-556
4. Kumari DNP, Haji TC, Keer V, Hawkey PM, Duncanson V and Flower E. Ventilation grilles as a potential source of methicillin-resistant *Staphylococcus aureus* causing an outbreak in an orthopaedic ward at a district general hospital. *Journal of Hospital Infection* 1998; 39: 127-133
5. Qian H, Li YG, Nielsen PV and Huang XH. Spatial distribution of infection risk of SARS transmission in a hospital ward. *Building and Environment* 2009; 44:1651-1658
6. HTM 03-01. Heating and ventilation systems, Health Technical Memorandum: 03-01: Specialised ventilation for healthcare premises. Department of Health, Leeds, UK, 2007.

7. NHS Sustainable Development Unit. Saving Carbon, Improving Health. NHS Carbon Reduction Strategy for England, Cambridge, 2009
8. Ko G, Burge HA, Nardell EA and Thompson KM. Estimation of Tuberculosis Risk and Incidence under Upper Room Ultraviolet Germicidal Irradiation in a Waiting Room in a Hypothetical Scenario. *Risk Analysis* 2001; 21(4): 657-673
9. Noakes CJ, Khan A, Gilkeson CA. Optimizing Upper-Room UVGI Systems for Infection Risk and Energy. In *ASHRAE IAQ 2013: Environmental Health in Low Energy Buildings*, the proceedings of 17th ASHRAE IAQ Conference, Vancouver, 15-18th October 2013; Paper 53, 385-394
10. Sharp G. The Effects of Ultraviolet Light on Bacteria Suspended in Air. *Journal of Bacteriology* 1940; 38: 535-547.
11. Sommer HE and Stokes J. Studies on Air-Borne Infection in a Hospital Ward: I. The Effect of Ultraviolet Light on Cross-Infection in an Infants Ward. *The Journal of Pediatrics* 1942; 21(5): 569-576.
12. Kowalski W. Ultraviolet Germicidal Irradiation Handbook. Springer, Heidelberg, 2009. ISBN 978-3-642-01998-2.
13. Riley RL and Permutt S. Room air disinfection by ultraviolet irradiation of upper air. *Archives of Environmental Health* 1971; 22: 208-219.
14. Peccia J, Werth HM, Miller SL and Hernandez MT. Effects of relative humidity on the ultraviolet induced inactivation of airborne bacteria. *Aerosol Science and Technology* 2001; 35: 728-740.
15. Xu PJ, Peccia J, Fabian P, Martyny JW, Fennelly KP, Hernandez M and Miller SL. Efficacy of ultraviolet germicidal irradiation of upper-room air in inactivating airborne bacterial spores and mycobacteria in full-scale studies. *Atmospheric Environment* 2003; 37: 405-419.
16. Noakes CJ, Fletcher LA, Beggs CB, Sleigh PA, and Kerr KG. Development of a numerical Model to Simulate the Biological Inactivation of Airborne Microorganisms in the Presence of Ultraviolet Light. *Journal of Aerosol Science* 2004; 35: 489-507.
17. Escombe AR, Moore DAJ, Gilman RH, Navincopa M, Ticona E, Mitchell B, Noakes CJ, Martínez C, Sheen P, Ramirez R, Quino W, Gonzalez A, Friedland JS and Evans CA. Upper-room ultraviolet light and negative air ionization to prevent tuberculosis transmission, *PLOS medicine* 2009; 6(3): e1000043
18. Sung M and Kato S. Estimating the germicidal effect of upper-room UVGI system on exhaled air of patients based on ventilation efficiency. *Building and Environment* 2011; 46: 2326-2332.
19. Gilkeson CA and Noakes CJ. Application of CFD Simulation to Predicting Upper-Room UVGI Effectiveness. *Photochemistry and Photobiology* 2013; 89(4):799-810
20. Noakes CJ, Beggs CB and Sleigh PA. Modelling the Performance of Upper Room Ultraviolet Germicidal Irradiation Devices in Ventilated Rooms: Comparison of Analytical and CFD Methods. *Indoor and Built Environment* 2004; 13(6): 477-488

21. Alani A, Barton IE, Seymour MJ and Wrobel LC. Application of Lagrangian particle transport model to tuberculosis TB bacteria UV dosing in a ventilated isolation room. *International Journal of Environmental Health Research* 2001; 11: 219-228.
22. Noakes CJ, Sleigh PA, Fletcher LA and Beggs CB. Use of CFD Modelling to Optimise the Design of Upper-Room UVGI Disinfection Systems for Ventilated Rooms. *Indoor and Built Environment*. 2006; 15(4): 347-356.
23. Sung M and Kato S. Method to Evaluate UV Dose of Upper-Room UVGI System Using the Concept of Ventilation Efficiency. *Building and Environment* 2010; 45: 1626-1631.
24. Zhu S, Srebric J, Rudnick SN, Vincent RL and Nardell EA. Numerical Investigation of Upper-Room UVGI Disinfection Efficacy in an Environmental Chamber with a Ceiling Fan. *Photochemistry and Photobiology* 2013; 89(4):782–791
25. Gilkeson CA, Camargo-Valero MA, Pickin LE, Noakes CJ Measurement of Ventilation and Airborne Infection Risk in Large Naturally Ventilated Hospital Wards. *Building and Environment* 2013; 65:35-48
26. Escombe, AR, Oeser CC, Gilman RH, Navincopa M, Ticona E, Pan W, Martinez C, Chacaltana J, Rodrigues R, Moore DAJ, Friedland JS, Evans CA. Natural ventilation for the prevention of airborne contagion. *Plos Medicine* 2007;4(2):309-317.
27. Qian H, Li Y, Seto WH, Ching P, Ching WH, Sun HG. Natural ventilation for reducing airborne infection in hospitals. *Building and Environment* 2010;45(3):559-565.
28. Gilkeson CA, Noakes CJ, Sleigh PA, Khan MAI and Camargo-Valero MA. Simulating pathogen transport within a naturally ventilated hospital ward. *World Academy of Science, Engineering and Technology* 2011;79: 119-125.
29. Roache PJ. Perspective: A Method for Uniform Reporting of Grid Refinement Studies. *Journal of Fluids Engineering* 1994; 116:405-413.
30. Launder BE, Reece GJ and Rodi W. Progress in the Development of a Reynolds-Stress Turbulence Closure. *Journal of Fluid Mechanics* 1975; 68(3): 537-566.
31. King M-F, Noakes CJ, Sleigh PA, Camargo-Valero MA Bioaerosol deposition in single and two-bed hospital rooms: A numerical and experimental study. *Building and Environment* 2013; 59:436-447
32. Wright NG, Hargreaves DM. The use of CFD in the evaluation of UV treatment systems. *Journal of Hydroinformatics* 2001; 3: 59-70
33. Narayanan A, Toropov VV, Wood AS and Campean IF. Simultaneous Model Building and Validation with Uniform Designs of Experiments. *Engineering Optimization* 2007; 39(5): 497-512.
34. Audze P, Eglais V. New Approach to Planning Out of Experiments. *Problems of Dynamics and Strength. Zinatne* 1977; 35:104-107.
35. Zhou L and Haghghat F Optimization of ventilation system design and operation in office environment, Part I: Methodology. *Building and Environment* 2009; 44: 651-656.

36. Khan MAI, Noakes CJ, Toropov VV. Development of a numerical optimization approach to ventilation system design to control airborne contaminant dispersion and occupant comfort. *Building Simulation: An International Journal* 2012; 5(1): 39-50
37. Gilkeson CA, Toropov VV, Thompson HM, Wilson MCT, Foxley NA and Gaskell PH. Multi-Objective Aerodynamic Shape Optimization of Small Livestock Trailers. *Engineering Optimization* 2013; 45(11): 1309-1330.
38. Choi KK, Youn BS, Yang RJ. Moving Least Square Method for Reliability-Based Design Optimization. In *Proceedings of 4th World Congress of Structural and Multidisciplinary Optimization*, 4–8 June 2001, Dalian, China. CD-ROM proceedings (WCSMO-4). Dalian: Liaoning Electronic Press, 1–6.
39. Toropov VV, Schramm A, Sahai A, Jones R, Zeguer T. Design Optimization and Stochastic Analysis Based on the Moving Least Squares Method. In *Proceedings of the 6th World Congress of Structural and Multidisciplinary Optimization*, 30 May–3 June 2005, Rio de Janeiro, Brazil, edited by J. Herskovits, S. Matorche, and A. Canelas. Rio de Janeiro: COPPE Publications, (CD-ROM).
40. Madsen JI, Shyy W and Haftka RT. Response surface techniques for diffuser shape optimization. *American Institute of Aeronautics and Astronautics Journal* 2000; 38(9): 1512:1518.
41. Burman J and Gebart BR. Influence from numerical noise in the objective function for flow design optimisation. *International Journal of Numerical Methods for Heat & Fluid Flow* 2001; 11(1): 6-19.
42. Press WH, Teukolsky SA, Vetterling WT and Flannery BP. *Numerical Recipes in C++ : The Art of Scientific Computing*. 3rd ed. Cambridge: Cambridge University Press, 2007.
43. Loeppky J, Sacks J and Welch WJ. Choosing the sample size of a computer experiment: a practical guide. *Technometrics* 2009; 51: 366-376.
44. Beggs CB, Noakes CJ, Sleight PA, Fletcher LA and Kerr KG. Methodology for determining the susceptibility of airborne microorganisms to irradiation by an upper-room UVGI system. *Journal of Aerosol Science* 2006; 37(7): 885-902.
45. NIOSH. *Environmental Control for Tuberculosis: Basic Upper-Room Ultraviolet Germicidal Irradiation Guidelines for Healthcare Settings*. Centers for Disease Control and Prevention, National Institute for Occupational Safety and Health, Washington DC, 2009.
46. ASHRAE Handbook: HVAC Applications. Chapter 60, Ultraviolet Air and Surface Treatment. American Society of Heating, Refrigeration and Air Conditioning Engineers, Atlanta, 2011.